J. Fluid Mech. (1994), *vol.* 264, *pp.* 59–80

A numerical and theoretical study of the first Hopf bifurcation in a cylinder wake

By JAN DUŠEK, PATRICE LE GAL AND PHILIPPE FRAUNIÉ†

Institut de Mécanique Statistique de la Turbulence, 12, Av. Général Leclerc, 13003 Marseille, France

(Received 23 February 1993 and in revised form 17 September 1993)

The first Hopf bifurcation of the infinite cylinder wake is analysed theoretically and by direct simulation. It is shown that a decomposition into a series of harmonics is a convenient theoretical and practical tool for this investigation. Two basic properties of the instability allowing the use and truncation of the series of harmonics are identified: the lock-in of frequencies in the flow and separation of the rapid timescale of the periodicity from the slow timescale of the non-periodic behaviour. The Landau model is investigated under weak assumptions allowing strong nonlinearities and transition to saturation of amplitudes. It is found to be rather well satisfied locally at a fixed position of the flow until saturation. It is shown, however, that no truncated expansion into a series of powers of amplitude can account correctly for this fact. The validity of the local Landau model is found to be related to the variation of the form of the unstable mode substantially slower than its amplification. Physically relevant characteristics of the Hopf bifurcation under the assumption of separation of three timescales – those of the periodicity, amplification and deformation of the mode – are suggested.

1. Introduction

Experimental measurements, as well as results of numerical simulations of the instabilities at a fixed spatial point of various incompressible flows, seem to confirm very accurately the Landau model of the Hopf bifurcation (Landau & Lifshitz 1959). As a result, practically all experimental and numerical investigations of the Hopf bifurcation in incompressible fluid flows have been carried out in the framework of this model. Experimental investigations of the Landau model have concentrated on the cases of an infinite cylinder wake (Mathis, Provansal & Boyer 1987; Sreenivasan, Strykowski & Olinger 1987; Strykowski & Sreenivasan 1990) and a round jet (Raghu & Monkewitz 1991). Complete numerical studies have not been reported so far; however, numerous data are available concerning the Strouhal number of the cylinder wake at low Reynolds numbers (Karniadakis & Triantafyllou 1989; Braza, Chassaing & Ha Minh 1986) or the critical Reynolds number (Jackson 1987). The typical behaviour of the Hopf bifurcation has been found also at the second bifurcation in the cylinder wake, corresponding to the transition to tridimensionality (Karniadakis & Triantafyllou 1992).

Since the introduction of the Landau model to explain the transition to instability of fluid flows an uncertainty has been characterizing its interpretation in systems of an infinite number of degrees of freedom. The problem appears because the model:

† Present address: LSEET, Université de Toulon et du Var, BP 132, 83954 La Garde, Cédex, France.

$$\frac{\mathrm{d}u}{\mathrm{d}t} = (\gamma + \mathrm{i}\omega)\, u - (C_r + \mathrm{i}C_i)\, |u|^2 u \tag{1}$$

does not concern the spatial variables of the instability.

The linear analysis allows the complex constant $\gamma + \mathrm{i}\omega$ to be understood as an eigenvalue of the linearized Navier–Stokes operator. The physical meaning of γ and ω is that of the amplification rate and the angular frequency, respectively, of oscillations having infinitesimal amplitudes. These constants are thus global (global in that sense that they are the same at all points of the flow) characteristics of the unstable global (Huerre & Monkewitz 1990) mode. To determine these characteristics it is sufficient to place a probe at an arbitrary point of the flow and record the time evolution of any flow characteristic. (In the cylinder wake the first bifurcation corresponds to the symmetry breaking in the plane perpendicular to the cylinder axis, the usual characteristic chosen is thus the transverse velocity in the flow axis.)

This is not the case for the constant $C_r + \mathrm{i}C_i$ of the Landau model. To see this it is sufficient to consider the saturation amplitude (corresponding to $\mathrm{d}|u|/\mathrm{d}t = 0$), given by $(\gamma/C_r)^{\frac{1}{2}}$. This amplitude varies in space, which implies that the 'constant' C_r varies in space.

To avoid this problem it has been suggested that the amplitude normalized with respect to the saturation amplitude should be introduced (see e.g. Raghu & Monkewitz 1991):

$$\tilde{u} = u(C_r/\gamma)^{\frac{1}{2}},$$

which yields an equation of the form

$$\frac{\mathrm{d}\tilde{u}}{\mathrm{d}t} = (\gamma + \mathrm{i}\omega)\, \tilde{u} - \gamma\left(1 - \mathrm{i}\frac{\Delta\omega}{\gamma}\right)|\tilde{u}|^2 \tilde{u},$$

where $\Delta\omega \equiv -\gamma C_i/C_r$ stands for the increase of angular frequency which occurs during amplification of the amplitude to saturation:

$$\Delta\omega = \omega_{sat} - \omega.$$

This approach reduces considerably the predictability of the model however. Whereas the linear model (1) (without the cubic term) predicts the true value of the amplitude at any time, as long as the nonlinear terms remain negligible, the reduced model no longer provides the possibility of predicting more than the percentage of the saturation amplitude reached at a given time moment. Moreover, the constant $\Delta\omega$ is not *a priori* independent of the spacial position. The fact that $\Delta\omega$ seems to be actually a global constant is non-trivial and is certainly related to the nonlinear phenomenon of lock-in states observed in wakes (Karniadakis & Triantafyllou 1989; Li, Sun & Roux 1992). Thus, the validity of the Landau model needs to be investigated and explained.

Limitations of the Landau model theory appear also when the higher harmonics appearing at the instability are studied. This phenomenon can be described accurately near the onset of the instability (in the weakly nonlinear case). Some theoretial papers tackle this problem in parallel flows (Benney 1960; Gaster 1968; Stewartson & Stuart 1971). The method used, consisting in developing the solution of the Navier–Stokes equations into a power series of some parameter, most frequently the oscillation amplitude, have been summarized by Herbert (1983). These perturbation methods are, however, unable to describe the bifurcation completely up to the saturation of the

amplitude. The theory presented by Herbert (1983) consists in casting the fundamental unstable mode in the form

$$\varphi_1(.,t) = A(t) \sum_{m=0}^{\infty} \sum_{m=0}^{\infty} \phi_{1,m}(.)\, A(t)^{2m}, \tag{2}$$

the dot standing for all relevant spatial variables (which can be one to three, depending on the case described). The Landau model then arises by truncating the above expression at $m = 1$. It is clear that this truncation holds only for small amplitudes. At saturation the first- and third-order terms ($m = 0$ and $m = 1$) become comparable, which means that higher-order terms can no longer be neglected. Hence the validity of the Landau model up to saturation cannot be considered as a trivial consequence of the perturbation theory. In the same way, (2) predicts correctly that the fundamental mode deforms as the amplitudes grow. However, as indicated by our direct simulations of the cylinder wake, this deformation is quite substantial and cannot be accounted for by a limited series expansion.

In this paper we develop a nonlinear theory based on the separation of timescales characteristic of the Hopf bifurcation. We show that, at least in the cylinder wake close to the instability threshold, there is a substantial difference between the timescale defined by the period of wake oscillations, that defined by the amplification rate and that characterizing the deformation of the mode. If the oscillation period is substantially smaller than the timescale of the amplification, it is possible to obtain, in a natural way, a rapidly converging decomposition of the unstable perturbation into a series of harmonics. We present this development in §2. In the same section we reconsider the Landau model on the basis of such a development. One interpretation consists in reducing it to the system with a single degree of freedom represented by the fundamental mode. In §3 we present results of numerical simulations of the infinite-cylinder wake. We find that the theory presented in §2 holds except the proposed interpretation of the Landau model. In §4 we suggest therefore a generalized version of the model obtained by truncating the development of the unstable perturbation at the second harmonic. We show that the fact that the complex constant $C = C_r + \mathrm{i}C_i$ appears to be independent of time is due to the slow timescale of deformation of the mode as compared to the timescale of its amplification. This constant remains, however, dependent on the spatial position. As a result the full characterization of the Hopf bifurcation within the framework of this model cannot be reduced to space-independent constants.

2. Theory

2.1. *Linear theory*

The usual linear theories (Drazin & Reid 1981) of the onset of instabilities in fluid flows are based on linearized Navier–Stokes equations. To simplify our analysis let us limit ourselves to the case of a two-dimensional flow described in the stream function formulation by a single equation:

$$\frac{\partial \nabla^2 \psi}{\partial t} + \frac{\partial \psi}{\partial y}\frac{\partial \nabla^2 \psi}{\partial x} - \frac{\partial \psi}{\partial x}\frac{\partial \nabla^2 \psi}{\partial y} - \frac{1}{Re}\nabla^4 \psi = 0 \tag{3}$$

where ∇^2 stands for the Laplacian operator and the velocities (u, v) can be expressed as the partial derivatives of ψ via

$$u = \frac{\partial \psi}{\partial y}, \quad v = -\frac{\partial \psi}{\partial x}.$$

Equation (3) is made dimensionless with respect to a characteristic length and velocity. In our case we shall be concerned with an unconfined flow past a circular cylinder. The characteristic length will be thus the cylinder diameter D and the characteristic velocity the inflow velocity at infinity U_∞, so that $Re = U_\infty D/\nu$. Moreover if $\tilde{x}$, $\tilde{y}$, $\tilde{u}$, $\tilde{v}$ and $\tilde{t}$ are the variables describing the coordinates, velocities and time in, say, metres, metres per second and seconds, the dimensionless variables x, y, u, v and t are defined as follows:

$$x = \frac{\tilde{x}}{D}, \quad y = \frac{\tilde{y}}{D}, \quad u = \frac{\tilde{u}}{U_\infty}, \quad v = \frac{\tilde{v}}{U_\infty}, \quad t = \frac{\tilde{t}U_\infty}{D}.$$

Let us assume the flow field ψ_0, the solution of equation (3), to be unstable for a given Reynolds number Re. The instability is characterized by the existence of a solution of the form

$$\psi = \psi_0 + \varphi, \tag{4}$$

where φ is a perturbation of ψ_0 having a trend to amplification. If we insert (4) into (3) and neglect the nonlinear terms we arrive at the equation

$$\frac{\partial \nabla^2 \varphi}{\partial t} + \mathscr{L}[\psi_0]\varphi = 0 \tag{5}$$

where $\mathscr{L}[\psi_0]$ is the following linear operator:

$$\mathscr{L}\varphi \equiv U\frac{\partial \nabla^2 \varphi}{\partial x} + V\frac{\partial \nabla^2 \varphi}{\partial y} - \nabla^2 U\frac{\partial \varphi}{\partial x} - \nabla^2 V\frac{\partial \varphi}{\partial y} - \frac{1}{Re}\nabla^4 \varphi, \tag{6}$$

and where U and V are, respectively, the streamwise and transverse velocity of the unperturbed flow field:

$$U = \frac{\partial \psi_0}{\partial y}, \quad V = -\frac{\partial \psi_0}{\partial x}.$$

Let us assume the instability to be initiated by an infinitely small perturbation φ. To give rise to the instability, this perturbation has to be linearly dependent on an eigenfunction of the problem:

$$(\mathscr{L} + \lambda \nabla^2)\phi = 0 \tag{7}$$

corresponding to an eigenvalue λ having a positive real part $\mathrm{Re}(\lambda)$.

The eigenvalue problem (7) is not fully defined unless the boundary conditions are specified. Depending on the boundary conditions the spectrum of the operator (6) may be either discrete or continuous. In the case of wakes or jets the eigensolutions can be assumed to be confined in space (i.e. at least square-integrable along with their partial derivatives up to a given order), which yields a discrete spectrum (see e.g. Jackson 1987). The physical meaning of such eigensolutions is that of waves having a time-independent envelope. A wide class of problems defined on infinite domains does not have any discrete spectrum. Such is the case of parallel flows. In that case the boundary

conditions have to express the physical situation corresponding to travelling wave packets the form of which is to be defined at infinity. For parallel flows such waves are simply plane waves throughout the whole domain. In general, the boundary conditions may express that the solutions behave asymptotically like plane waves far up- and downstream. Such solutions are, of course, no longer square-integrable and describe a continuous spectrum parametrizable by the wavenumber of the asymptotic wave.

The discrete spectrum case presents a special theoretical interest as it includes instabilities arising in confined domains or instabilities in flows with stationary (and easily experimentally controllable) boundary conditions in the absence of non-stationary external forcing. As we have already remarked, the case of wakes belongs to this class of flows. For this reason, we shall assume the perturbation φ to satisfy the following boundary conditions on the boundary $\partial\Omega$ of the domain Ω:

$$\varphi|_{\partial\Omega} = 0, \quad \nabla\varphi|_{\partial\Omega} = 0. \tag{8}$$

A compatible regularity requirement consists in assuming the space of solutions to be square-integrable along with their partial derivatives of order one and two. Such functions satisfying the boundary conditions (8) form the Sobolev space $\mathscr{H}_0^{(2)}$.

The operator (6), as well as the boundary conditions (8), being real, λ is an eigenvalue corresponding to the eigenfunction ϕ if and only if the complex conjugate $\bar{\lambda}$ is the eigenvalue corresponding to the eigenfunction $\bar{\phi}$. The eigenvalues being discrete, we can assume that sufficiently close to the instability threshold, there exists one and only one pair of eigenvalues with a positive real part. Let us denote these eigenvalues $\lambda_\pm^{(0)}$:

$$\lambda_\pm^{(0)} = \gamma \pm \mathrm{i}\omega$$

with

$$\gamma \geqslant 0, \quad \omega > 0. \tag{9}$$

The equality in condition (9) corresponds to the threshold of the instability. The eigenfunctions corresponding to these eigenvalues will be denoted $\phi_\pm^{(0)}$:

$$[\mathscr{L} + (\gamma \pm \mathrm{i}\omega)\nabla^2]\phi_\pm^{(0)} = 0. \tag{10}$$

Let us consider again the initial perturbation φ to belong to $\mathscr{H}_0^{(2)}$ as a function of spatial variables. As only the part proportional to $\phi_+^{(0)}$ and $\phi_-^{(0)}$ will be amplified while the projections onto other eigenvalues will decay rapidly, the initial perturbation can be assumed to be a linear combination of $\phi_\pm^{(0)}$. We shall have

$$\varphi = a_+\varphi_+^{(0)} + a_-\varphi_-^{(0)} \tag{11}$$

where

$$\varphi_+^{(0)} = \mathrm{e}^{(\gamma+\mathrm{i}\omega)t}\phi_+^{(0)}, \quad \varphi_-^{(0)} = \overline{\varphi_+^{(0)}}. \tag{12}$$

The observed perturbation being real we have, moreover, $a_- = \overline{a_+}$ and we shall denote simply $a_+ \equiv a$. The coefficient a expresses the magnitude of the initial perturbation and is thus assumed to be infinitely small.

2.2. *Nonlinear theory*

It is clear that, owing to the exponentially increasing factor $\mathrm{e}^{\gamma t}$, the solution (11), (12) of the linear problem will finally grow so much that the nonlinear terms will no longer remain negligible. To investigate the nonlinear effects it is necessary to consider the full nonlinear equation for the perturbation φ:

$$\frac{\partial\nabla^2\varphi}{\partial t} + \mathscr{L}[\psi_0]\varphi + \mathscr{B}(\varphi,\varphi) = 0 \tag{13}$$

containing the nonlinear term

$$\mathscr{B}(\varphi,\varphi) \equiv \frac{\partial\varphi}{\partial y}\frac{\partial\nabla^2\varphi}{\partial x} - \frac{\partial\varphi}{\partial x}\frac{\partial\nabla^2\varphi}{\partial y}. \tag{14}$$

Sufficiently close to the instability threshold, the amplification rate γ is substantially smaller than the angular frequency ω of oscillations with small amplitudes: $\gamma \ll \omega$. As long as the perturbation remains small, its temporal evolution is characterized by oscillations with angular frequency ω slowly amplified in time with the amplification rate γ and modulated in space by the eigenmodes of the linear problem (10) as expressed by equations (11), (12). It is thus useful to introduce two timescales (e.g. Newell & Whitehead 1969; Stewartson & Stuart 1971). One, expressed by the variable t, will correspond to the rapid oscillations with period $2\pi/\omega$. The other, expressed by the variable s, will summarize all the other, substantially slower, variations of the perturbation, the main one being that corresponding to the amplification of the amplitudes. The solution of (10) can then be written as

$$\varphi(t) = \chi(t,t), \tag{15}$$

$\chi(s,t)$ being the real solution of the equation

$$\frac{\partial\nabla^2\chi}{\partial s} + \frac{\partial\nabla^2\chi}{\partial t} + \mathscr{L}[\psi_0]\chi + \mathscr{B}(\chi,\chi) = 0 \tag{16}$$

on $\mathscr{H}_0^{(2)}$, periodic with period $2\pi/\omega$ as a function of t, satisfying the initial condition

$$\chi(s,t) \underset{s\to 0}{\sim} a_+ \mathrm{e}^{\gamma s + \mathrm{i}\omega t}\phi_+^{(0)} + a_- \mathrm{e}^{\gamma s - \mathrm{i}\omega t}\phi_-^{(0)}. \tag{17}$$

(As far as the spatial coordinates are concerned, all equalities are expressed in $\mathscr{H}_0^{(2)}$.) The introduction of the variable s amounts to nothing more than a simple mathematical trick allowing the fact that the time dependence is dominated by periodic oscillations to be accounted for. Equation (15) expresses the relation between the new function $\chi(s,t)$ which is periodic in the second argument and the original, in general aperiodic, function φ. It should be read so that s is replaced by the function $s(t) \equiv t$. The t-derivative of the right-hand side of (15) thus obviously yields the sum of the first two terms of (16), which, together with (13), explains the equality (15). The variable s thus accounts for any deviation of the final solution (15) from the periodicity of χ in t and therefore the generality of the formulation is conserved.

The function $\chi(s,t)$ can now be expanded into a Fourier series:

$$\chi(s,t) = \sum_{n=-\infty}^{+\infty} c_n(s)\,\mathrm{e}^{\mathrm{i}n\omega t}, \tag{18}$$

the coefficients of which are $\mathscr{H}_0^{(2)}$ functions on Ω depending, moreover, on the variable s. The function $\chi(s,t)$ being real, the coefficients of its Fourier series satisfy

$$c_n(s) = \overline{c_{-n}(s)}. \tag{19}$$

The Fourier components $c_n(s)$ satisfy the infinite system of equations coupled via the nonlinear terms:

$$\frac{\partial\nabla^2 c_n}{\partial s} + (\mathscr{L}[\psi_0] + \mathrm{i}n\omega\nabla^2)\,c_n + \sum_{k=-\infty}^{+\infty} \mathscr{B}(c_k, c_{n-k}) = 0. \tag{20}$$

The initial condition (17) takes the following form:

$$c_n(s) \underset{s\to 0}{\sim} a\,\mathrm{e}^{\gamma s}\phi_+^{(0)}\,\delta_{n,1} + \bar{a}\,\mathrm{e}^{\gamma s}\phi_-^{(0)}\,\delta_{n,-1}, \tag{21}$$

$\delta_{m,n}$ being the Kronecker symbol.

For small amplitudes the expansion (18) is characterized by a decrease of the modes c_n proportional to $|a|^n$. This behaviour of higher harmonics close to the onset of instability is used for example by the perturbation theory of Herbert (1983). Indeed, the modes $c_{\pm 1}$ being the only ones having a non-zero initial condition, all the other modes become non-zero via the nonlinear term represented by the sum on the right-hand side of (20). Equation (21) can be written as

$$c_{\pm 1}(s) \underset{s\to 0}{\sim} O(|a|),$$

and the modes corresponding to $n \neq \pm 1$ satisfying for $s \to 0$

$$\frac{\partial \nabla^2 c_n}{\partial s} + (\mathscr{L}[\psi_0] + \mathrm{i}n\omega\nabla^2)\,c_n + \mathscr{B}(c_1, c_{n-1}) + \mathscr{B}(c_{-1}, c_{n+1}) + \mathscr{B}(c_{n-1}, c_1) + \mathscr{B}(c_{n+1}, c_{-1}) = 0. \tag{22}$$

The nonlinear term thus becomes non-zero first for $n = -2, 0, 2$, yielding

$$c_{\pm 2}(s), c_0(s) \underset{s\to 0}{\sim} O(|a|^2).$$

Taking into account progressively all the modes of the order $O(|a|^k)$ with $k \leqslant n-1$ we find:

$$c_n(s) \underset{s\to 0}{\sim} O(|a|^n).$$

To see if the same hierarchy of harmonics remains valid for large values of s, let us consider the case of $s \to \infty$. In this case, experiments and numerical simulations show that the amplitudes of oscillations reach saturation and become periodic with an angular frequency ω_∞ different from ω. This experimental fact can be formulated in the form of the following assumption:

Assumption 1:

$$\varphi_\infty(t) = \sum_{n=-\infty}^{+\infty} b_n\,\mathrm{e}^{\mathrm{i}n\omega_\infty t}.$$

In what follows we shall test this assumption by a direct numerical simulation of the cylinder wake.

If we compare the expansion of Assumption 1 to (15) and (18) we get

$$c_n(s) \underset{s\to\infty}{\sim} b_n\,\mathrm{e}^{\mathrm{i}n\Delta\omega s},$$

where

$$\Delta\omega = \omega_\infty - \omega.$$

The saturation amplitudes of the individual harmonics are then solutions of the system

$$(\mathscr{L}[\psi_0] + \mathrm{i}n\omega_\infty\nabla^2)\,b_n + \sum_{k=-\infty}^{+\infty} \mathscr{B}(b_k, b_{n-k}) = 0.$$

We expect the saturation frequency to be not very different from ω.

Assumption 2:

$$\gamma \ll \omega, \quad \Delta\omega \ll \omega.$$

As we saw in §1, the angular frequency increase $\Delta\omega$ is proportional to the amplification rate, proportional itself to the deviation of the Reynolds number from its critical value. Thus Assumption 2 amounts to assuming only weakly supercritical Reynolds numbers:

$$\frac{Re - Re_{crit}}{R_{crit}} \ll 1.$$

Close to the threshold of the instability the eigenvalues (10) are the only ones approaching the imaginary axis $\mathrm{Re}(\lambda) = 0$. The value of $\Delta\omega$ being small, the values $\lambda = 0, \pm 2\omega_\infty$ are thus far away from the spectrum of the linear operator $\mathscr{L}[\psi_0]$. The linear operators on the left-hand sides of the equations of the system above (for $n \neq \pm 1$) are thus invertible. The norms of the inverse operators are roughly proportional to $1/[(n-1)\omega]$. If the magnitude of amplitudes of the fundamental modes $n = \pm 1$ remains smaller than 1 (the velocities remain smaller than the velocities of the unperturbed flow), we still have small higher harmonics obeying the relation

$$b_n \sim O(|b_{\pm 1}|^n).$$

As the result we find that:

COROLLARY:

$$\forall s, \quad c_n(s) \sim O(|c_{\pm 1}|^n). \tag{23}$$

The relation (23), if satisfied and if the norms of the fundamental modes $c_{\pm 1}$ can be considered as small parameters, allows the system of equations (20) to be reduced to a small number of equations (see Bayly, Orszag & Herbert 1988).

2.3. *The Landau model*

The assumptions of the preceding subsection are very weak. Let us now study additional assumptions yielding the Landau model.

If we assume the amplitudes of the fundamental mode to be small enough we can limit the number of harmonics in the system (20). If we consider (22) for $n = -2, 0, 2$ then Assumptions 1 and 2 allow us to assume that the evolution in the variable s is very slow compared to the angular frequency ω:

$$\left\| \frac{\partial \nabla^2 c_n}{\partial s} \right\| \ll \omega \|\nabla^2 c_n\|,$$

the norm being understood in $L^2(\Omega)$. The first term in (22) is thus negligible for all modes except the fundamental one. This is the well-known phenomenon of slave modes (Manneville 1990).

Let us try to test the following additional assumption consisting in assuming the form of the fundamental mode not to vary during the amplification from small amplitudes to the saturation:

Assumption L:

$$\forall s, \quad c_1 = A(s)\,\phi_+^{(0)}, \quad c_{-1} = \overline{c_1}. \tag{24}$$

Assumption L implies that

$$c_0 = |A(s)|^2\,\eta_0, \quad c_2 = A(s)^2\,\eta_2, \quad c_{-2} = \overline{c_2}, \tag{25}$$

the functions η_0 and η_2 being given by

$$\mathscr{L}[\psi_0]\eta_0+\mathscr{B}(\phi_+^{(0)},\phi_-^{(0)})+\mathscr{B}(\phi_-^{(0)},\phi_+^{(0)})=0, \tag{26}$$

$$(\mathscr{L}[\psi_0]+2i\omega\nabla^2)\eta_2+\mathscr{B}(\phi_+^{(0)},\phi_+^{(0)})=0. \tag{27}$$

If we insert (24)–(27) into (22) (with $n=1$) neglecting the terms of order higher than three (in the sense of (23)) and taking into account (10) we obtain

$$\left(\frac{\partial A}{\partial s}-\gamma A(s)\right)\nabla^2\phi_+^{(0)}+|A(s)|^2A(s)\beta=0, \tag{28}$$

where β is a function of the position in space given by

$$\beta=\mathscr{B}(\eta_0,\phi_+^{(0)})+\mathscr{B}(\phi_+^{(0)},\eta_0)+\mathscr{B}(\eta_2,\phi_-^{(0)})+\mathscr{B}(\phi_-^{(0)},\eta_2). \tag{29}$$

Whereas $A(s)$ is a global amplification factor of the fundamental mode, the solution of (28) depends on the spatial position unless

$$\forall(x,y)\in\Omega,\quad \beta(x,y)=C\nabla^2\phi_+^{(0)}(x,y), \tag{30}$$

where $C=C_r+iC_i$ is a complex constant. Equation (30) is equivalent to Assumption L – equation (24). Then A is, indeed, a complex function of a single real variable satisfying the equation

$$\frac{dA}{ds}-\gamma A(s)+C|A(s)|^2A(s)=0, \tag{31}$$

which is the Landau model after separation of oscillations with the angular frequency corresponding to small amplitudes of the fundamental mode $e^{i\omega t}$. Separating the amplitude $|A(s)|$ from the phase of $A(s)$ we can write in the usual way

$$\frac{d|A|}{ds}-\gamma|A(s)|+C_r|A(s)|^3=0 \tag{32}$$

and

$$\Delta\omega(s)+C_i|A(s)|^2=0, \tag{33}$$

yielding the following values at saturation:

$$|A_\infty|=(\gamma/C_r)^{\frac{1}{2}},\quad \Delta\omega_\infty=-C_i\gamma/C_r.$$

At saturation, the fundamental mode takes the following form:

$$\varphi_{+,\infty}(x,y,t)=(C_r/\gamma)^{\frac{1}{2}}\phi_+^{(0)}(x,y)\,e^{i(\omega+\Delta\omega_\infty)t}. \tag{34}$$

Under Assumption L the Landau model thus applies to the global amplitude A of the unstable mode. The value of the Landau constant C is dependent on the normalization of the mode $\phi_+^{(0)}$ but independent of the spatial position. Assumption L corresponds in fact to the central manifold theory by stating that the instability can be described by projecting onto the unstable mode $\phi_+^{(0)}$. The accuracy of this assumption will be checked in the following section.

3. Test of the theory by a numerical simulation of a cylinder wake

To check the assumptions formulated in §§2.2 and 2.3 we investigated numerically the wake of an infinite cylinder slightly above the first Hopf bifurcation threshold. The two-dimensional simulation was performed using the Nekton code† based on a

† Copyright © 1991 by creare.x, Inc., Hanover, New Hampshire, USA, Nekton is a registered trademark of Nektonics, Inc. and the Massachussetts Institute of Technology.

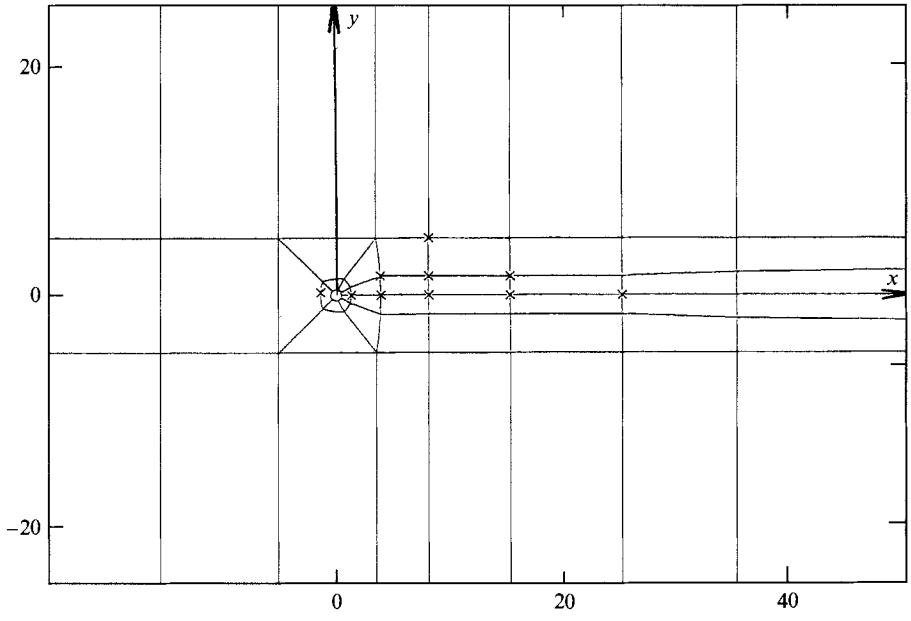

FIGURE 1. Decomposition of the domain into spectral elements (axes labelled in cylinder diameters).

Point	x	y
1	1.35	0
2	3.92	0
3	8.00	0
4	15.00	0
5	25.00	0
6	−1.47	0.23
7	3.87	1.67
8	8.00	1.67
9	15.00	1.67
10	8.00	5.00

TABLE 1. Position of points (in cylinder diameter units) at which the time evolution of the unstable mode was investigated (x, streamwise direction; y, transverse direction, both expressed in cylinder diameters). The origin lies in the cylinder centre.

spectral element spatial discretization (Patera 1984). A substantial effort has been made to optimize the discretization to obtain as realistic results as possible. The detailed discussion of the discretization optimization and the analysis of the accuracy obtained is not the purpose of the present paper as qualitatively the same results can be obtained with a much less accurate discretization. Let us, however, remark that the results presented in this section can actually be guaranteed to be of a better than 1 % accuracy in such basic quantities as the critical Reynolds number (found to be about 46.1), the amplification rate and the Strouhal number.

The domain decomposition into spectral elements is represented in figure 1. The ten crosses in figure 1 mark the position of 10 points at which the temporal evolution of the unstable mode has been investigated. The coordinates of these points, expressed in cylinder diameters with respect to the position of the cylinder centre, are given in

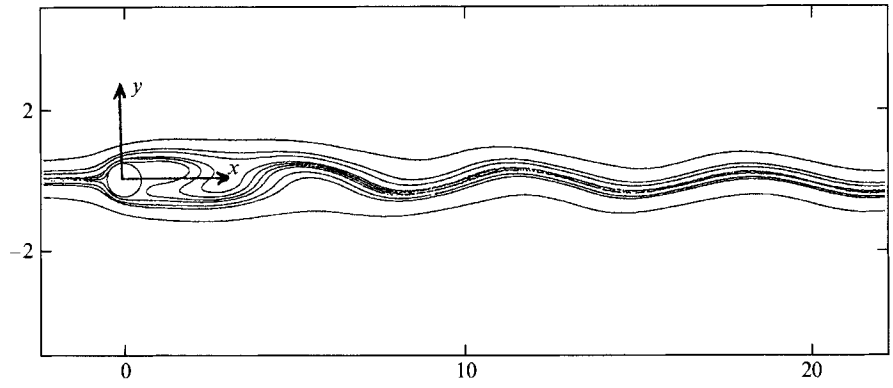

FIGURE 2. Cylinder wake at saturation ($Re = 48$, axes labelled in cylinder diameters).

table 1. The boundary conditions have been chosen in the following way: a uniform velocity profile at the inflow boundary, a periodicity condition at the lateral boundaries and a free outflow condition at the outflow boundary. Ten collocation points in each spatial direction of a spectral element have been taken.

The present calculation was performed at $Re = 48$, i.e. only slightly above the critical value of 46. The overall aspect of the flow obtained at saturation is visualized by several streamlines in figure 2. In figure 3(*a–c*) we show the time evolution of the transverse velocity at points 3, 6 and 10. It is clearly seen that the mode is, indeed, global with the same time evolution in the flow axis downstream and upstream of the cylinder as well as far off the wake axis. As explained below, the signals of the transverse velocity at the points lying at the flow axis contain no even harmonics, whereas at the points lying off the axis the zeroth harmonic is present and, in the same way as the first one, develops in time. This explains the asymmetric growth in figure 3(*c*).

Let us consider first Assumptions 1, 2 and their Corollary (23). According to these statements the spectra of the signals obtained at points 1–10 should be:

(i) discrete (Assumption 1);

(ii) not very different for small and big amplitudes (Assumption 2);

(iii) dominated by a small number of basic harmonics ($n = 1, 2, 3$) (Corollary).

In figure 4(*a–e*) we present the logarithmic spectra of signals obtained at points 1, 3, 5, 8, and 10 corresponding to the first and second half of the computation time interval, i.e. to small amplitudes and saturation amplitudes, respectively. The graphs represent the decadic logarithm of the modulus of the Fourier transform:

$$F[v](\nu) = \frac{1}{\Delta t}\int_0^{\Delta t} v(t)\,\mathrm{e}^{-2\pi \mathrm{i}\nu t}\,\mathrm{d}t$$

of the transverse velocity v as a function of the Strouhal number. (A unit of the vertical axis corresponds to one order of magnitude.) It can be seen that Assumptions 1, 2 and their Corollary are well satisfied. Let us remark that the Strouhal number expressing the dimensionless frequency of the fundamental harmonic is 0.12 which in agreement with experimental results (see e.g. Williamson 1989).

It should be explained why the second harmonics are absent in the spectra of signals obtained at the flow axis. To see this let us note that the symmetry of the unperturbed flow implies that the operator (6) commutes with the operator of inversion of the y-axis defined as

$$\mathscr{P}[f](x, y) \equiv f(x, -y).$$

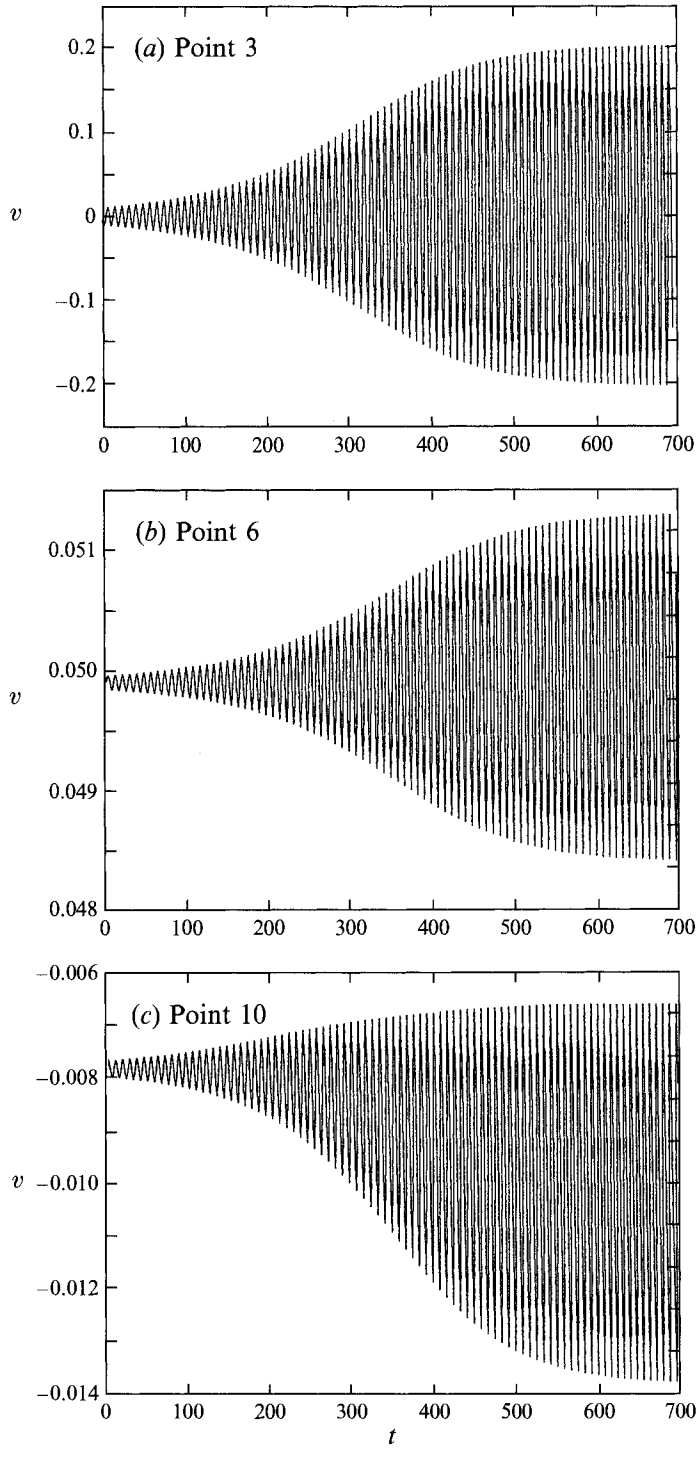

FIGURE 3. Time evolution of the transverse velocity at: (*a*) point 3 ($x = 8$, $y = 0$); (*b*) point 6 ($x = -1.47$, $y = 0.23$); (*c*) point 10 ($x = 8$, $y = 5$). Point 10 lies above the flow axis ($y > 0$), the signal is asymmetric.

Written formally $$\mathscr{P}\mathscr{L}[\psi_0] = \mathscr{L}[\psi_0]\mathscr{P}.$$

Similarly, relation (14) allow us to write

$$\forall \xi, \eta, \quad \mathscr{P}\mathscr{B}(\xi, \eta) = -\mathscr{B}(\mathscr{P}\xi, \mathscr{P}\eta).$$

If we apply the operator $\mathscr{P}$ to both sides of each of (20) we then easily find that if the sequence of modes $\{c_n\}_{n=-\infty}^{\infty}$ is a solution of system (20) then the sequence $\{(-1)^{n+1}\mathscr{P}[c_n]\}_{n=-\infty}^{\infty}$ is also a solution. The uniqueness of the solution of (20) below the next bifurcation threshold then yields

$$c_n(x, -y) = (-1)^{n+1} c_n(x, y). \tag{35}$$

Equation (35) shows that the odd modes are symmetric and the even modes are antisymmetric. As a result the even modes of the stream function vanish on the symmetry axis. Owing to the relations following (3) the transverse velocity v possesses the same symmetry properties as the stream function whereas the longitudinal velocity – the y-derivative of the stream function – has symmetric even modes and antisymmetric odd modes. This explains, in particular, the well-known fact that a probe placed in the flow axis indicates a frequency of the longitudinal velocity two times too high.

Let us finally consider the Landau model interpretation suggested in §2.3. Figure 5 shows the form of the transverse velocity profile along the flow axis downstream of the cylinder for small amplitudes and at saturation. It is immediately seen that the form of the mode varies rather substantially. Let us note that figure 5 shows also that the streamwise wavelength of the vortex street far downstream of the cylinder is 7.7 cylinder diameters, which is in agreement with the value given by Williamson (1989) for the same Reynolds number. This value combined with that obtained for the Strouhal number yields a phase velocity of 0.92.

Though this figure shows how poorly Assumption L is satisfied we further analysed (31). Using the Hilbert transform with an appropriate window (Croquette & Williams 1989; Kolodner & Williams 1990; Le Gal 1992) it is possible to separate the amplitude and the phase of the signal to analyse (32) and (33) directly. The results of this analysis are shown in figure 6, where the envelope of oscillations is compared to the positive part of the signal at point 1, and in figure 7, representing the variation of the frequency (Strouhal number) in time. We determined the coefficients of the linear relation between the logarithmic time derivative and the square of the amplitude:

$$\frac{\mathrm{d}|A|}{\mathrm{d}s}/|A(s)| = \gamma - C_r|A(s)|^2 = 0 \tag{36}$$

and between the angular frequency and the square of the amplitude:

$$\tilde{\omega}(s) = \omega - C_i|A(s)|^2 = 0, \tag{37}$$

by the least-squares method. As we have already pointed out, to define unambiguously the Landau constant $C_r + \mathrm{i}C_i$ we have to normalize the linear mode $\phi_+^{(0)}$. The true dependence of the logarithmic derivative of the amplitude and the angular frequency on the square of the amplitude for point 1 is represented in figure 8. (The normalization in figure 8 is arbitrary.) The linearity is obviously rather accurately satisfied. The easiest way to normalize the linear mode was to set its value to 1 at one of the investigated points. For this purpose we chose point 5 ($x_0 = 25$, $y_0 = 0$), at which the

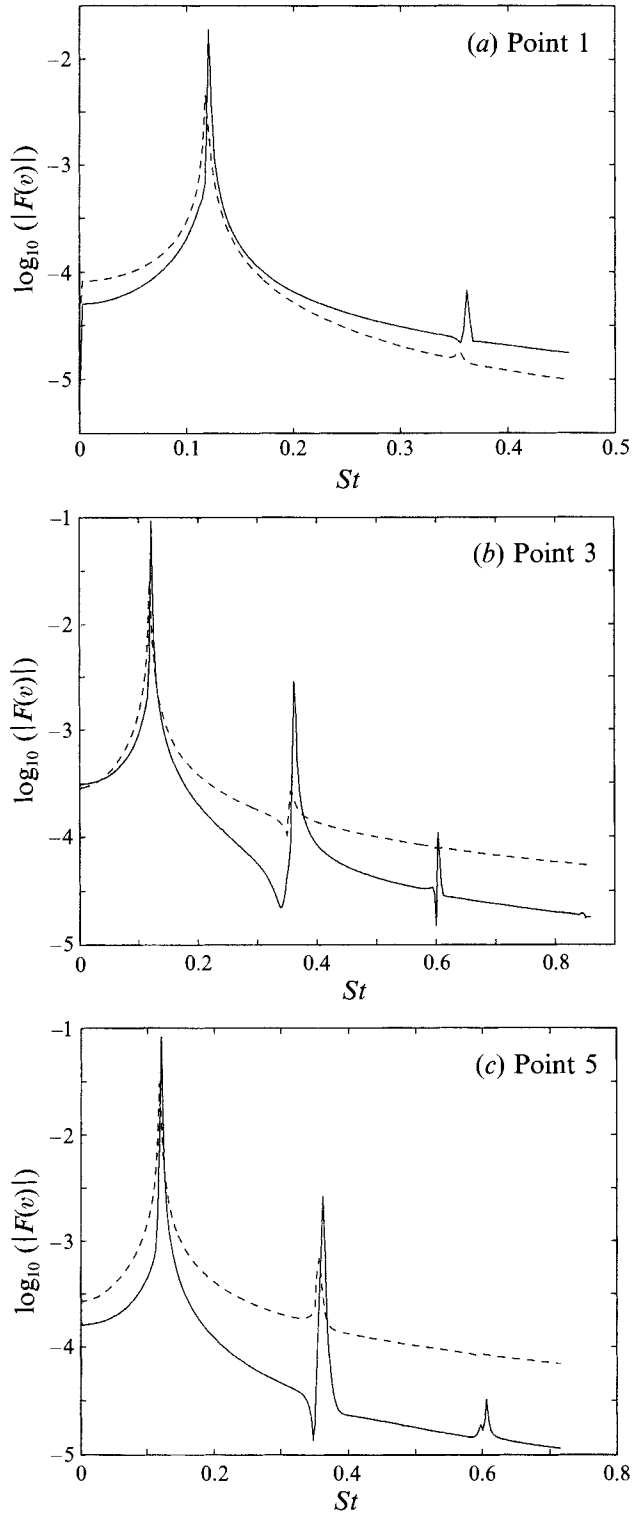

FIGURE 4 (*a–c*). For caption see facing page.

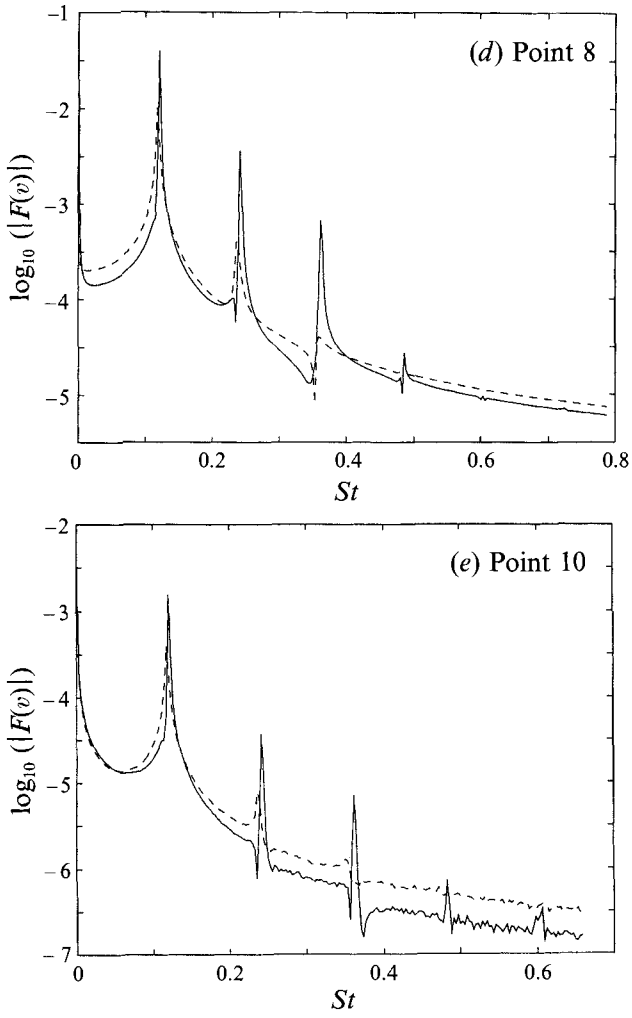

FIGURE 4. Spectra ($\log_{10}$ of the absolute value of the Fourier transform) of the transverse velocity $v = \tilde{v}/U_\infty$: for small amplitudes (dashed line) and at saturation (full line). The horizontal axis is labelled in Strouhal number values. (*a*) Point 1: the first peak corresponds to the fundamental harmonic, the second one to the third harmonic. The shift of frequency between the peaks of the dashed line and the full line is clearly visible. (*b*) Point 3: the first and third harmonics for both lines are visible. At saturation the fifth and seventh harmonic can be distinguished. (*c*) Point 5: the first, third and fifth (at saturation only) harmonics are visible. (*d*) Point 8: at saturation all the harmonics $n = 1, 2, 3, 4, 5, 6$ are visible. (*e*) Point 10: the first five harmonics are visible at saturation.

infinitesimal mode has maximum amplitudes (among the 10 chosen points), Equation (36) integrated in time at a fixed point (x, y) yields

$$a_v(x, y, s) = [a_{v,\infty}^{-2} + (a_{v,0}^{-2} - a_{v,\infty}^{-2})\,\mathrm{e}^{-2\gamma s}]^{-\frac{1}{2}},$$

$a_v(x, y, s)$ being the amplitude of the v-velocity in the point (x, y) at the time s. The infinitesimal amplitude corresponds to the extrapolation to $s \to -\infty$. The normalized amplitude will thus be defined as

$$A(t) = a_v(x, y, t)\,K(x, y),$$

where

$$K(x, y) = \left[\frac{a_{v,0}^{-2}(x, y) - a_{v,\infty}^{-2}(x, y)}{a_{v,0}^{-2}(x_0, y_0) - a_{v,\infty}^{-2}(x_0, y_0)}\right]^{\frac{1}{2}}.$$

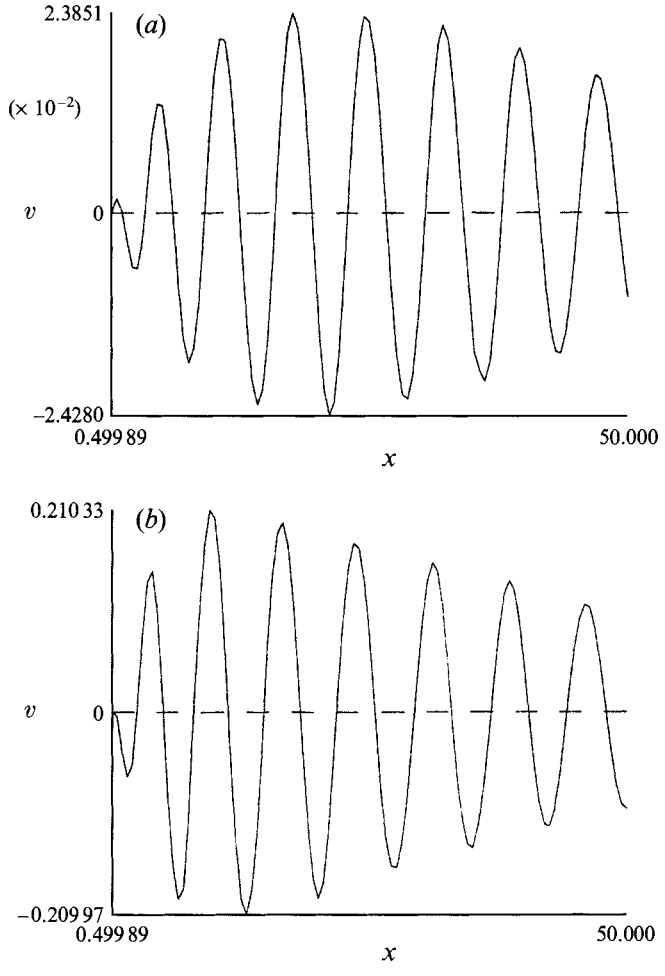

FIGURE 5. Transverse velocity profile ($v = \tilde{v}/U_\infty$ *vs.* $x = \tilde{x}/D$) along the wake axis ($y = 0$) downstream of the cylinder (*a*) for small amplitudes (maximal transverse velocity amplitude: 0.024) and (*b*) at saturation (maximal transverse velocity amplitude: 0.21).

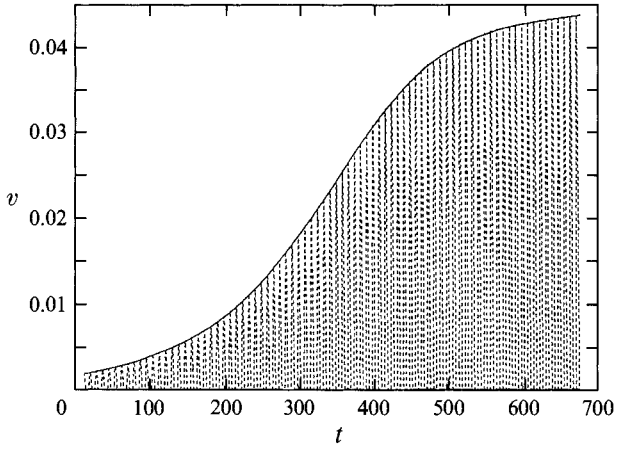

FIGURE 6. Comparison of the envelope of oscillations obtained by Hilbert transformation (full line) and of the analysed signal at point 1. (Only the positive part of the signal is shown.)

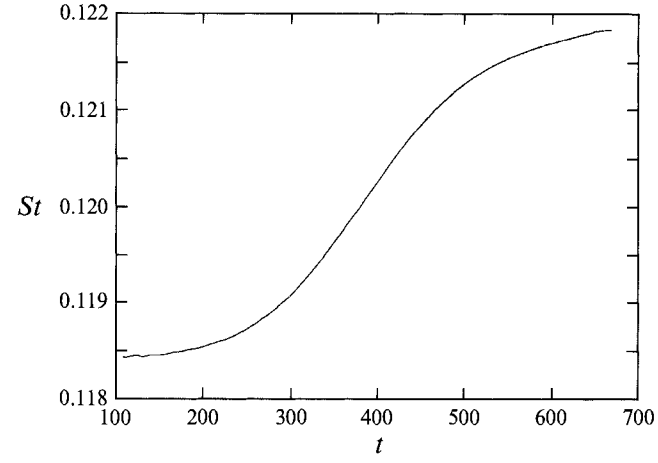

FIGURE 7. Time evolution of the Strouhal frequency.

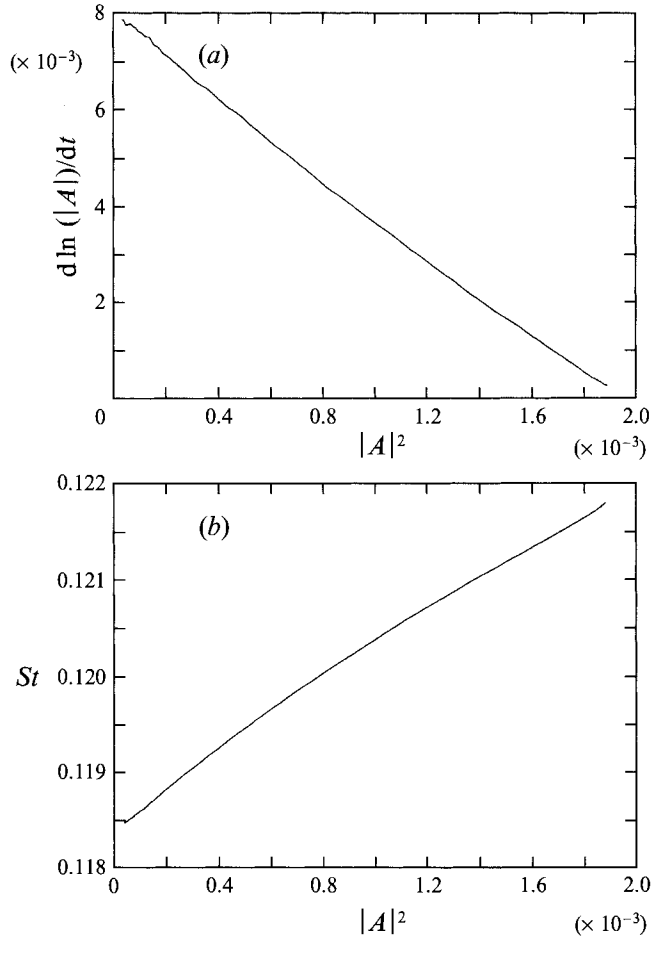

FIGURE 8. (*a*) Logarithmic time derivative of the amplitude of the dimensionless transverse velocity *vs.* square of the amplitude; (*b*) Strouhal number *vs.* square of the amplitude.

Point	γ	C_r	ω	C_i	C_i/C_r	$\Delta\omega$
1	0.007934	0.526	0.7412	−1.423	−2.707	0.02148
2	0.007938	0.176	0.7410	−0.474	−2.701	0.02144
3	0.007933	0.137	0.7403	−0.371	−2.700	0.02142
4	0.007972	0.173	0.7391	−0.467	−2.704	0.02156
5	0.007884	0.246	0.7383	−0.684	−2.774	0.02187
6	0.007903	15.577	0.7414	−42.218	−2.710	0.02142
7	0.007966	0.5740	0.7410	−1.542	−2.686	0.02140
8	0.007914	0.307	0.7406	−0.832	−2.709	0.02144
9	0.007921	0.255	0.7405	−0.689	−2.701	0.02138
10	0.007931	7.007	0.7410	−19.044	−2.718	0.02156

TABLE 2. Characteristics of the Landau model for the dimensionless transverse velocity in the wake of a circular cylinder at the Reynolds number $Re = 48$

The results of the analysis of the coefficients of the Landau model are assembled in table 2. We remark that the results presented concerning the value of the ratio C_i/C_r (equal to -2.7) are in good agreement with experiment (Sreenivasan *et al.* 1987).

In table 2 we can see that the amplification rates γ and the angular frequency ω extrapolated to infinitesimal amplitudes, as well as the angular frequency variation $\Delta\omega$ at saturation (hence also the ratio C_i/C_r), are very accurately identical at all the investigated points. By contrast, the coefficients C_r and C_i related to the amplitudes normalized as indicated above are far from constant. The general trend is for the gradients of the envelope of oscillations to increase, high values of the constant C_r meaning a small relative amplification at the saturation. It is seen that the mode is amplified most of all near its maximum and much less at the periphery: upstream of the obstacle and far from the wake axis. Moreover, the maximum of the mode approaches the cylinder as the amplitudes are amplified. This is an experimentally observed trend (Mathis 1983).

If we consider the deviation of the curves in figure 8 from linearity we might be tempted to try to obtain a more accurate model by determining the next-order term of the expansion in a series of powers of $|A(s)|^2$. In the introduction we, however, argued that the expansion in a series of powers of the amplitude cannot account for the behaviour of the oscillations up to the saturation. An explanation of the nonlinearity of the curves in figure 8 will be given in the next section in terms of the form deformation of the unstable mode.

4. Slow deformation of the mode form and the Landau model

As we have seen in the preceding section, the Landau model cannot be interpreted exactly as describing the temporal evolution of the global amplitude of the unstable mode. It is, nevertheless, interesting to understand why the increase of amplitudes of oscillations of the transverse velocity recorded at various points of the flow follows so accurately the Landau model. Let us, for this purpose, take again the system (20). We have seen (see the Corollary in §2.2) that it is possible to limit the system to a few of harmonics. Let us consider just $n = -2, -1, 0, 1, 2$. The equation corresponding to the fundamental mode can then be written as

$$\frac{\partial \nabla^2 c_1}{\partial s} + (\mathscr{L}[\psi_0] + i\omega\nabla^2)\, c_1 + \mathscr{B}(c_1, c_0) + \mathscr{B}(c_{-1}, c_2) + \mathscr{B}(c_0, c_1) + \mathscr{B}(c_2, c_{-1}) = 0. \quad (38)$$

To close the system it is necessary to add the following equations ($c_{-1} = \overline{c_1}$):

$$\mathscr{L}[\psi_0]\, c_0 + \mathscr{B}(c_1, \overline{c_1}) + \mathscr{B}(\overline{c_1}, c_1) = 0, \tag{39}$$

$$(\mathscr{L}[\psi_0] + 2\mathrm{i}\omega\nabla^2)\, c_2 + \mathscr{B}(c_1, c_1) = 0. \tag{40}$$

If we solve (39), (40) with respect to c_0 and c_2 and insert into (38) we arrive at a single equation for the fundamental harmonic:

$$\frac{\partial \nabla^2 c_1}{\partial s} - \gamma c_1 + (\mathscr{L}[\psi_0] + \gamma + \mathrm{i}\omega)\, c_1 + \bar{\mathscr{B}}(c_1) = 0,$$

where $\bar{\mathscr{B}}$ is a nonlinear operator yielded by the mentioned reduction of the system (38)–(40). If we switch to the velocity representation:

$$a_1 \equiv [a_{u,1}, a_{v,1}],$$

where
$$a_{u,1}(x, y, s) = \frac{\partial c_1}{\partial y}(x, y, s), \quad a_{v,1}(x, y, s) = -\frac{\partial c_1}{\partial x}(x, y, s)$$

this equation assumes the form:

$$\frac{\partial a_1}{\partial s} - \gamma a_1 + (\mathrm{L}[\psi_0] + \gamma + \mathrm{i}\omega)\, a_1 + \mathrm{B}(a_1) = 0, \tag{41}$$

where L and B are the respective linear and nonlinear operators in the velocity representation. We do not need the explicit form of these operators. For what follows it is sufficient to use such representation-independent properties as conservation of eigenvalues of the linear operator L and the property of the nonlinear operator:

$$\mathrm{B}(A\varphi) = A|A|^2\, \mathrm{B}(\varphi) \tag{42}$$

valid for any spatial function φ and any complex constant A. This last property is immediately obtained using the bi-linearity of the operator $\mathscr{B}$ and (38)–(40). Let us write the second component of (41) formally as

$$\frac{\partial a_{v,1}(x, y, s)}{\partial s} - \gamma a_{v,1}(x, y, s) + C_{v,1}(x, y, s)\, |a_{v,1}(x, y, s)|^2\, a_{v,1}(x, y, s) \tag{43}$$

with
$$C_{v,1}(x, y, s) = \left. \frac{(\mathrm{L}[\psi_0] + \gamma + \mathrm{i}\omega)\, a_{v,1} + \mathrm{B}(a_1)_v}{|a_{v,1}|^2\, a_{v,1}} \right|_{(x,y,s)}. \tag{44}$$

The index 1 indicates that we refer to the fundamental harmonic and v refers to the v-component. (A similar analysis can be made for higher harmonics too.) As can be seen from (44) the function $C_{v,1}(x, y, s)$ depends on the time variable s. This explains the nonlinear behaviour of the curves in figure 8. It remains to understand why the time dependence of $C_{v,1}(x, y, s)$ is weak. To see this let us separate the amplification from the form deformation of the mode by writing

$$a_1(x, y, s) = A(s)\, \alpha_1(x, y, s), \tag{45}$$

where $\alpha_1(x, y, s)$ has a fixed normalization (e.g. a fixed value at reference point) and the complex factor $A(s)$ is set to be equal to 1 for $s = 0$ ($\alpha_1(x, y, s)$ corresponds to the infinitesimal mode for $s \to 0$.) Figure 5 shows that while the amplitudes of the oscillations are multiplied by a factor of 10, the form of the unstable mode changes much less. If we take as a criterion the displacement of the maximum of the mode, the

rate of this change is about 30–40%. (The maximum lies at the point $x = 21$ for small amplitudes and at the point $x = 13.3$ at saturation.) As a result

$$\frac{\mathrm{d}\ln(A(s))}{\mathrm{d}s} \gg \frac{\partial \ln|a_1(x,y,s)|}{\partial s}. \tag{46}$$

If we insert (45) into (44) and use (42), we see that the amplification factor $A(s)$ can be simplified between the second term of the numerator and the denominator. As to the first term in the numerator, it is negligible as can be seen if we remember that for $s \to 0$ it is zero (the infinitesimal mode is the eigenmode corresponding to the eigenvalue $\gamma + \mathrm{i}\omega$) and, at the approach to saturation where the mode is deformed, it yields a term proportional to the very small factor $|A(s)|^{-2}$. As a result the only relevant term remaining in (44) is independent of the amplification factor $A(s)$ and thus, by (45), the logarithmic derivative of $C_{v,1}(x,y,s)$ with respect to s is proportional only to the logarithmic derivative of $a_1(x,y,s)$:

$$\frac{\mathrm{d}\ln(A(s))}{\mathrm{d}s} \gg \frac{\partial \ln|C_v(x,y,s)|}{\partial s}.$$

We can thus see that if:

Assumption 3: the variation of the form of the unstable mode is substantially slower than the amplification of its amplitude (see the inequality (46)), then the function $C_{v,1}(x,y,s)$ can be considered as independent of time (s).

If this is the case the real part of the spatial function $C_{v,1}(x,y)$ determines the saturation amplitude of the fundamental harmonic of the transverse velocity $a_{v,1,\infty}$ via

$$a_{v,1,\infty} \equiv |a_{v,1}(x,y,\infty)| = \left(\frac{\gamma}{\mathrm{Re}\,[C_{v,1}(x,y)]}\right)^{\frac{1}{2}}$$

and the ratio of the real and imaginary parts yields the increase of angular frequency:

$$\Delta\omega = -\gamma \frac{\mathrm{Im}\,[C_{v,1}(x,y)]}{\mathrm{Re}\,[C_{v,1}(x,y)]}.$$

Using these characteristics it is possible to write (43) in the following form:

$$\frac{\partial a_{v,1}(x,y,s)}{\partial s} - \gamma a_{v,1}(x,y,s) + \frac{\gamma}{a_{v,1,\infty}^2}\left(1 - \mathrm{i}\frac{\Delta\omega}{\gamma}\right)|a_{v,1}(x,y,s)|^2 a_{v,1}(x,y,s) = 0. \tag{47}$$

Whereas the real numbers γ, ω and $\Delta\omega$ are the same for the fundamental harmonic of each flow characteristic and for each spatial point of the flow, each component of the flow field is characterized by a specific function expressing its saturation amplitude at each point of the flow. To obtain a complete characterization of the bifurcation a vector of components representing the independent characteristics of the flow (e.g. both velocity components in two dimensions and the velocity formulation), has to be given.

The model presented in (47) is valid only if Assumptions 1–3 are satisfied. It is, however, more general than the classical interpretation of the Landau model and presents the following advantages:

(i) assumptions 1–3 do not exclude large amplitudes approaching saturation;
(ii) the model contains only directly measurable quantities;
(iii) the model is always accurate for both small and saturation amplitudes.

(At saturation (47) reduces to identity, for small amplitudes the coefficient of the nonlinear term becomes inaccurate but the term is negligible.)

5. Conclusions

We have analysed the behaviour of the cylinder wake at the first Hopf bifurcation. Numerous experimental and numerical results show that, at each point of the flow, the flow characteristics, such as the transverse velocity, follow very closely the Landau model. We have shown that the explanation cannot be based on a truncated development of the Navier–Stokes equations into a series of powers of the amplitude. Two basic phenomena explain the Landau-like behaviour of the unstable flow:

(i) the effect of lock-in states allowing the presence of only a single frequency in the flow after saturation and stabilization of the flow oscillations;

(ii) a deformation of the form substantially slower than the amplification of the unstable mode.

It appears that, if the assumptions formulated in §§2.2 and 4 are satisfied, the unstable mode is characterized by three real constants: the amplification rate and the angular frequency of infinitesimal oscillations and the increase of angular frequency at saturation, and by one real (in general vectorial) function in space describing the saturation amplitudes of the set of flow characteristics in a given representation of the flow at each point of the flow.

Expansion (18) might provide an interesting alternative for the numerical study of periodic flows (Carte, Fraunie & Dussouillez 1991). In the case of unstable flows, such as wakes, it would be of interest to explore how the number of harmonics dominating the oscillations increases with increasing Reynolds number. The signal clearly becomes more complicated higher above the threshold, which indicates that the fundamental harmonic is no longer dominant. However, it can be expected that the time evolution of the flow remains smooth, which would still imply a rapid convergence of its Fourier expansion. If this proves to be the case Assumption 1 will allow the reduction of the problem of computing the amplitudes at saturation to a finite set of steady equations. This would be of significant importance for the separation of effects due to the onset of a subsequent bifurcation.

REFERENCES

BAYLY, B. J., ORSZAG, S. A. & HERBERT, T. 1988 Instability mechanisms in shear-flow transition. *Ann. Rev. Fluid Mech.* **20**, 359.

BENNEY, D. J. 1960 A non-linear theory for oscillations in a parallel flow. *J. Fluid Mech.* **10**, 209.

BRAZA, M., CHASSAING, P. & HA MINH, H. 1986 Numerical study and physical analysis of the pressure and velocity fields in the near wake of a circular cylinder. *J. Fluid Mech.* **165**, 79.

CARTE, G., FRAUNIE, P. & DUSSOUILLEZ, P. 1991 An innovative algorithm for periodic flows calculation using a parallel architecture. Some Applications for unsteady aerodynamics. In *Sixth Intl Symp. on Unsteady Aerodynamics, Aeroacoustics and Aeroelasticity of Turbomachines and Propellers, Univ. Notre Dame, USA, Sept. 15–19*, 1991 (ed. H. M. Atassi). Springer.

CROQUETTE, V. & WILLIAMS, H. 1989 Non-linear waves of the oscillatory instability in finite convective rolls. *Physica* D **37**, 300.

DRAZIN, P. G. & REID, W. H. 1981 *Hydrodynamic Stability*. Cambridge University Press.

GASTER, M. 1968 Growth of disturbances in both space and time. *Phys. Fluids* **11**, 723.

HERBERT, T. 1983 On perturbation methods in nonlinear stability theory. *J. Fluid Mech.* **126**, 167.

HUERRE, P. & MONKEWITZ, P. A. 1990 Local and global instabilities in spatially developing flows. *Ann. Rev. Fluid Mech.* **22**, 473.

JACKSON, C. P. 1987 A finite-element study of the onset of vortex shedding in flow past variously shaped bodies. *J. Fluid Mech.* **182**, 23.

KARNIADAKIS, G. E. & TRIANTAFYLLOU, G. S. 1989 Frequency selection and asymptotic states in laminar wakes. *J. Fluid Mech.* **199**, 441.

KARNIADAKIS, G. E. & TRIANTAFYLLOU, G. S. 1992 The three-dimensional dynamics and transition to turbulence in the wake of bluff objects. *J. Fluid Mech.* **238**, 1.

KOLODNER, P. & WILLIAMS, H. 1990 Dispersive chaos. In *Proc. NATO Advanced Research Workshop on Nonlinear Evolution of Spatio-temporal structures in Dissipative Continuous Systems* (ed. F. H. Busse & L. Kramer). NATO Series B2.225, p. 73. Plenum.

LANDAU, L. D. & LIFSCHITZ, F. M. 1959 *Fluid Mechanics, Course of Theoretical Physics*, vol. 6. Pergamon.

LE GAL, P. 1992 Complex demodulation applied to the transition to turbulence of the flow over a rotating disk. *Phys. Fluids* A **4**, 2523.

LI, J., SUN, J. & ROUX, B. 1992 Numerical study of an oscillating fluid cylinder in uniform flow and in the wake of an upstream cylinder. *J. Fluid Mech.* **237**, 457.

MANNEVILLE, P. 1990 *Dissipative Structures and Weak Turbulence*. Academic.

MATHIS, C. 1983 Propriétés de vitesse transverses dans l'écoulement de Bénard von Kármán aux faibles nombres de Reynolds. Thèse, Université Aix-Marseille.

MATHIS, C., PROVANSAL, M. & BOYER, L. 1987 The Bénard–von Kármán instability: transient and forced regimes. *J. Fluid Mech.* **182**, 1.

NEWELL, A. C. & WHITEHEAD, J. A. 1969 Finite bandwidth, finite amplitude convection. *J. Fluid Mech.* **38**, 279.

PATERA, A. T. 1984 A spectral element method for fluid dynamics: Laminar flow in a channel expansion. *J. Comput. Phys.* **54**, 468.

RAGHU, S. & MONKEWITZ, P. A. 1991 The bifurcation of a hot round jet to limit-cycle oscillations. *Phys. Fluids* A **3**, 501.

SREENIVASAN, K. R., STRYKOWSKI, P. J. & OLINGER, D. J. 1987 Hopf bifurcation, Landau equation, and vortex shedding behind circular cylinders. In *Proc. Forum on Unsteady Flow Separation, ASME Applied Mechanics, Bio engineering and Fluid Engineering Conference, Cincinnati, Ohio, June 11–17, 1987*. ASME FED, Vol. 52.

STEWARTSON, K. & STUART, J. T. 1971 A non-linear instability theory for a wave system in plane Poiseuille flow. *J. Fluid Mech.* **48**, 529.

STRYKOWSKI, P. J. & SREENIVASAN, K. R. 1990 On the formation and suppression of vortex shedding at low Reynolds numbers. *J. Fluid Mech.* **218**, 71.

WILLIAMSON, C. H. K. 1989 Oblique and parallel modes of vortex shedding in the wake of a circular cylinder at low Reynolds numbers. *J. Fluid Mech.* **206**, 579.